Published online April 5, 2007

A Simple Technique for Measuring Wetting Front Depths for Selected Soils

R. R. Wells*
M. J. M. Römkens
USDA-ARS National Sedimentation Lab.
598 McElroy Dr.
Oxford, MS 38655

J.-Y. Parlange
Biological and Environmental Engineering
Cornell Univ.
Ithaca, NY 14853

David A. DiCarlo
USDA-ARS National Sedimentation Lab.
598 McElroy Dr.
Oxford, MS 38655

T. S. Steenhuis
Biological and Environmental Engineering
Cornell Univ.
Ithaca, NY 14853

S. N. Prasad
Dep. of Civil Engineering
Univ. of Mississippi
Oxford, MS 38677

The depth of the wetting front within a soil sample in infiltration measurements, especially in soils that develop cracks on drying, is difficult to ascertain simply and nondestructively. A technique was developed to determine wetting front locations on prepared soil beds, with a miniature penetrometer probe of the needle type, immediately following a simulated rainfall event. The method involves placing a 0.5-kg weight atop a miniature penetrometer probe and measuring the penetration depth of the probe relative to a known datum. Five texturally different soils were tested under similar laboratory conditions to evaluate this method. The penetrometer-based method provided accurate estimates of the wetting front position in laboratory simulated rainfall infiltration studies for clay, silty clay, and sandy clay soils that differed from visually observed depths by <1 mm. For the silt loam soils, however, this method underestimated mean wetting front depths by as much as 4 mm, with a standard deviation of 1.6 mm and 95% confidence limits of ±2.5 mm. The penetrometer method was especially useful for detailed characterization of wetting front depths in soils where wetting was highly variable or irregular (e.g., cracking clay soils).

Knowledge about wetting front locations is extremely useful in infiltration and irrigation studies. Nondestructive determination of water content in the soil profile has been performed with neutron probes (van Bavel et al., 1961), gamma- and x-ray techniques (van Bavel et al., 1957; Reginato and Jackson, 1971; Petrovic et al., 1982; DiCarlo et al., 1997), and time-domain reflectometry (TDR) probes (Fellner-Felldeg, 1969; Topp et al., 1980, 1982). Gravimetric measurements are destructive and not repeatable. Both neutron probes (Lawless et al., 1963) and TDR probes (Knight, 1992) take average soil water content measurements throughout a relatively large volume; therefore, sharp wetting fronts cannot be measured accurately (<20 mm), especially when the wetting front varies considerably with respect to horizontal distance. Gamma-ray techniques tend to produce significant errors in systems where the soil water content and bulk density increase or decrease simultaneously (Nofziger, 1978). X-ray techniques offer point measurements, but require specialized chambers and usually involve rather small soil volumes and are expensive (Crestana et al., 1985; Tollner et al., 1989; Liu et al., 1993).

We developed a method of measuring wetting front depths for texturally different soils using a low-cost, miniature cone-type penetrometer. Historically, cone penetrometers have been used to characterize soil strength, soil compaction, and mechanical impedance to root growth (Perumpral, 1987). The American Society of Agricultural Engineers (ASAE) has specified design standards for cone penetrometers (ASAE, 2006), which include the cone angle, base area, shaft length, and a constant penetration rate. We used a miniaturized version of this standard penetrometer method to measure wetting front depths in simulated rainfall infiltration studies with a series of soils including a swelling clay soil that forms cracks on drying.

As soil consistency (resistance to external forces) varies greatly as a function of water content (Hillel, 1980), at a given load, a cone penetrometer may penetrate soil behind the wetting front but not dry soil ahead of the wetting front. The major determinant of soil consistency is the soil's degree of wetness. Soils undergo rather dramatic changes in consistency as they transition from a dry state to saturation, from a hard and brittle solid to a sticky and viscous liquid. These transitions

Soil Sci. Soc. Am. J. 71:669–673
doi:10.2136/sssaj2005.0403
Received 13 Dec. 2005.
*Corresponding author (rrwells@ars.usda.gov).

Table 1. Soil description and textural classification.

Soil series	Soil classification	Percentage-size class			Bulk density†
		Clay	Silt	Sand	
		——— % ———			Mg m^{-3}
Dubbs	Typic Hapludalf	30	55	15	1.38
Forestdale	Typic Ochragualf	31	60	9	1.37
Grenada	Glossic Fragiudalf	18	78	4	1.39
Ruston	Typic Paleudult	20	3	77	1.38
Sharkey	Vertic Haplaquept	65	32	3	1.36

† Reported bulk densities reflect packed bulk densities.

are universally known as Atterburg limits. Tackett and Pearson (1965) used resistance methods to examine crust strength at various stages of simulated rainfall and concluded that resistance increased rapidly with small additions of clay.

The objective of this work was to develop a repeatable, high-resolution penetrometer-based method to quantify wetting front depths in soils that form cracks on drying. We (i) evaluated the accuracy of the technique to measure wetting front depths for five fine-textured soils packed in soil columns and (ii) demonstrated the method's utility in characterizing nonuniform wetting fronts that develop in clay soils.

MATERIALS AND METHODS

Soils and Sample Preparation

Five different soils were chosen to evaluate the efficacy of this method in determining wetting front penetrations. They were: the surface horizon material of a Dubbs silt loam (Typic Hapludalf), a Forestdale silty clay (Typic Ochragualf), a Grenada silt loam (Glossic Fragiudalf), a Sharkey clay (Vertic Haplaquept), and the Glauconitic parent material of a Ruston silt (Typic Paleudult) (Table 1). The soils were crushed and sieved to pass a screen with 2-mm openings. A single column was prepared for each soil except the Sharkey clay, for which two samples were prepared. The soils were uniformly packed to a depth of 60 mm in 260-mm inside diameter Plexiglas cylindrical containers. Packing was done in five incremental stages that contained approximately 0.9 kg of soil per layer. A duplicate cylindrical sample (Sharkey clay) was prepared to test this method for different wetting front depths by protecting part of the surface with hammock filter media (typically used in air filter applications) to prevent surface sealing and enhance infiltration. The center of the soil sample was covered with a 30 by 130 by 25.4 mm filter strip before the simulated rainfall.

A large sample box (765 by 800 by 300 mm) was used for measurements with the Sharkey clay soil only. Soil was uniformly packed in 22 increments, each containing approximately 11.3 kg of soil. The soil was placed on 80 mm of fine sand and had a depth of 220 mm. The initial bulk density of the soil was 1.35 Mg m^{-3}.

Water Application

All samples were subjected to 30 mm h^{-1} simulated rainfall with an energy rate of 27 J m^{-2} mm^{-1} of rain using the oscillating, 80/150 v-jet nozzle-type rainfall simulator described by Meyer and Harmon (1979). In both the cylinder tests and the large sample box, the prepared sample was placed on a recording balance in an inclined position with 2% slope to monitor the amount of rain infiltration. Excess rain was collected at the lower end of the sample by aspirating off accumulated rainwater through a port opening at the soil surface level in the cylinder experiments or by collecting runoff in a funnel in the large sample box. The duration of the simulated rainfall in the cylinder tests was adjusted for each soil sample to produce a cumulative infiltration amount of approximately 10.8 mm. The large sample box was subjected to three, 3-h simulated rainfall events. Each simulated rainfall event was followed by 24 h of ambient drying under controlled laboratory conditions (24°C), then by extended periods of accelerated drying with a fan blowing warm air over the soil surface for the purpose of generating cracks. Accelerated drying was accomplished by using a wind tunnel, a box fan, and five heat lamps. The box fan was placed 2 m behind and 200 mm above the surface of the sample and the heat lamps were placed 610 mm behind the box fan to slightly elevate the temperature of the air being forced over the sample.

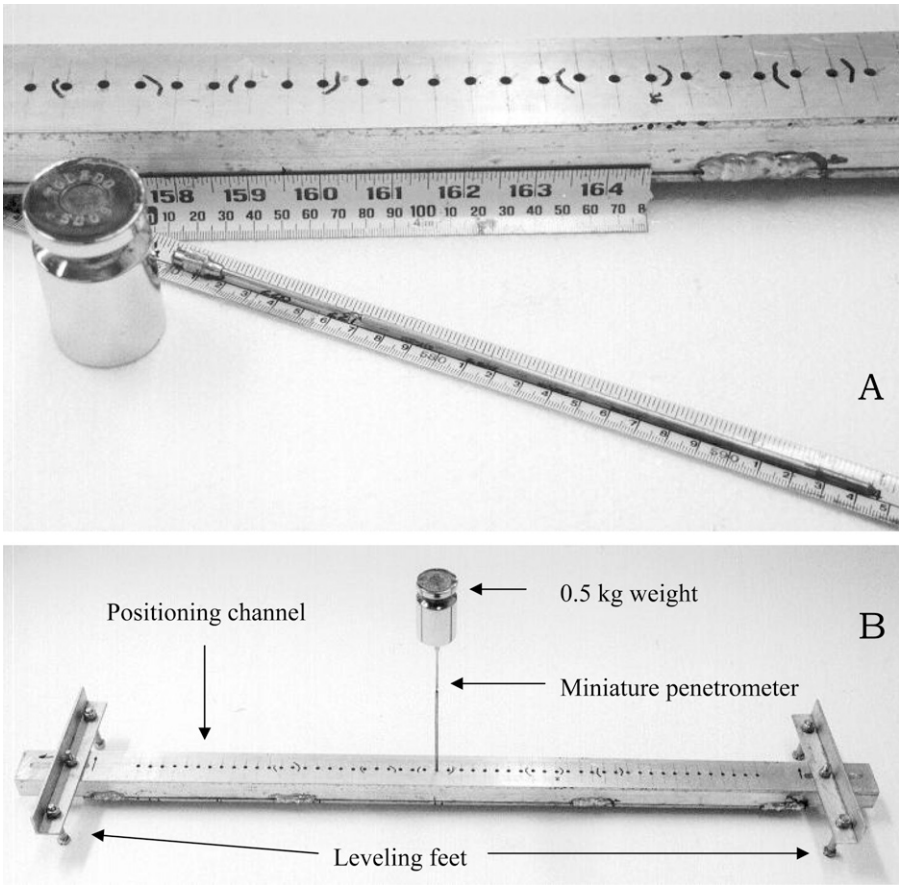

Fig. 1. (A) A view of the miniature penetrometer, the 0.5 kg loading weight, and the positioning channel. (B) A view of the experimental apparatus in loading mode.

Penetrometer

The experimental apparatus consisted of a miniature penetrometer, a 6061 T aluminum rectangular channel (44.5 by 25.4 mm), and a 0.5-kg weight (Fig. 1A). The cone-shaped tip of the penetrometer was machined from oil-hardened steel with a 60° total angle and a 3.05-mm-diameter base. The shaft consisted

of a stainless steel Becton-Dickinson YALE hypodermic needle (13G2 short bevel) of 2.54-mm diameter, machined into an oil-hardened steel rod with the same diameter. The tip, main shaft, and hypodermic needle were connected with liquid weld (JB Weld). Holes slightly larger than the base area of the cone of the penetrometer were drilled at 12.7-mm intervals along the centerline of the channel. Leveling feet were mounted on both ends of the channel. Figure 1B shows the experimental apparatus with the weight atop the penetrometer in a simulated loading mode. The surface elevation and depth of wetting fronts were obtained by measuring the height of the penetrometer above the channel as the tip of the penetrometer initially came into contact with the soil surface, and then again after the penetrometer came to rest under the 0.5-kg load. During the measurements, the 0.5-kg weight was balanced by hand atop the penetrometer after the surface elevation measurement was made. Care was taken to ensure vertical alignment before releasing the 0.5-kg weight. Penetrometer readings for the cylinder and box setups were precise to ±1 mm.

Cylinder Studies

Immediately following simulated rainfall, penetrometer measurements were made along single transects. The vertical datum in each test was set at the maximum soil surface elevation for that test. All penetration depth measurements were taken relative to the surface elevation at that particular location. A total of 21 probe measurements were made for each soil. Upon completion of the measurements, the columns were carefully dismantled, using a small knife to cut away excess soil, so that penetrometer holes were exposed along the measurement transect, and the depth of wetting could be measured by visual inspection at the location of the penetrometer reading. Change in color due to wetting was also used as a visual indicator of the wetting front position during the dismantling phase. Visual inspection accuracy was ±1 mm.

Box with Sharkey Clay

Immediately following the simulated rainfall, penetration measurements were made parallel to the surface drain and perpendicular to the surface slope of the soil box for a total of 52 probe measurements. The horizontal location of the measurements was arbitrarily chosen before the simulated rainfall. The penetrometer measurements disrupt the cracking pattern in the immediate area where the measurements are taken. For this reason, no measurements were made along the same transect in successive simulated rainfall events. The vertical datum for each set of surface elevation and wetting front penetration measurements was normalized to the measured maximum surface elevation before the first simulated rainfall event. The surface elevations before the first rainfall event were obtained with an automated infrared laser (Römkens et al., 1988; Wells et al., 2003). After each simulated rainfall event, the sample was allowed to dry for 24 h under ambient laboratory conditions, followed by accelerated drying. The large sample was not dismantled for independent visual measurements, as the sample was part of an ongoing investigation in cracking patterns. The measurements were only made for the first three rainfall events, then abandoned to allow the sample crack pattern to develop without disturbance from this type of measurement.

RESULTS AND DISCUSSION

The surface elevation measurement and depth of penetration into each soil in the cylinder tests are presented in Fig. 2. Penetration depths ranged from a minimum of 20 mm for the Sharkey clay to a maximum of 58 mm for the Grenada silt loam. Under similar conditions, the ranking from deep to shallow of the wetting penetration depth for the soils tested was: Grenada silt loam, Rustin silt, Dubbs silt loam, Forestdale silty clay, and Sharkey clay (Table 2). The penetration depths obtained with the penetrometer agreed very

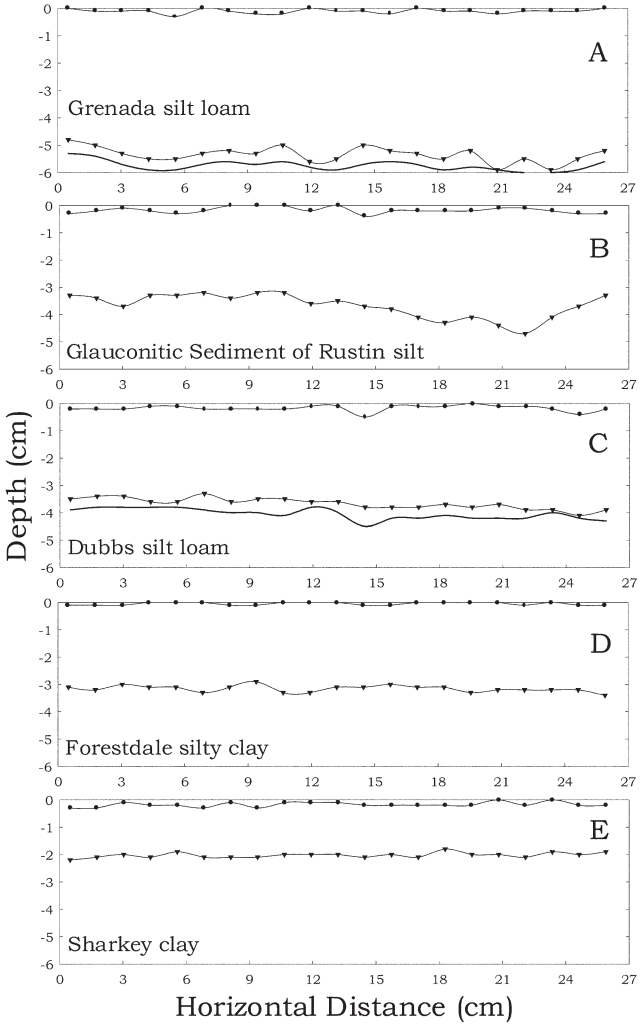

Fig. 2. Normalized surface elevation and penetration measurements from five field soils in order of decreasing penetration results. The solid line with circle symbols represents a spline fit through surface elevations and the solid line with the triangle symbols represents a spline fit through penetration depths. In (A) and (C), the solid line represents a spline fit through wetting front measurements made after dismantling, and in (B), (D), and (E), the penetration depth was very similar (<1 mm) to the wetting front depth.

Table 2. Mean wetting front depths, standard deviations, and paired *t*-tests for the penetrometer and visual measurements in the cylinder experiments.

Soil series	Mean wetting front depth measurements				
	Penetrometer	SD	Visual	SD	*P* value
	cm				
Dubbs	3.67	2.01	4.05	1.97	<0.0001
Forestdale	3.16	1.21	3.16	1.21	<0.0001
Grenada	5.34	2.80	5.74	1.86	<0.0001
Ruston	3.68	4.45	3.68	4.45	<0.0001
Sharkey	2.02	0.94	2.02	0.94	<0.0001

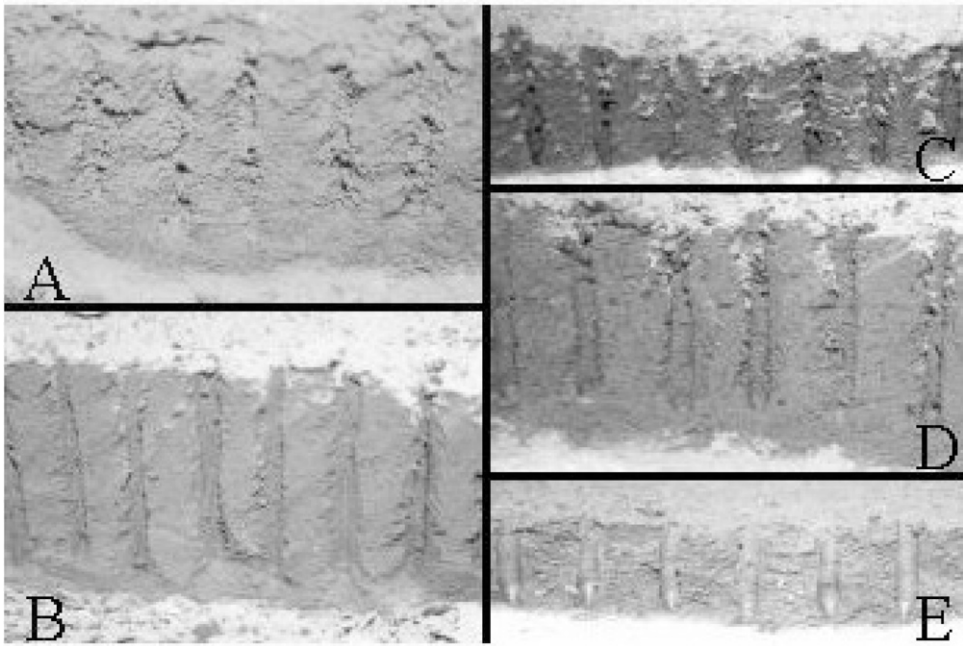

Fig. 3. Photographs of the dismantled soil samples after penetration: (A) Glauconitic sediment of Ruston silt, (B) Grenada silt loam, (C) Forestdale silty clay, (D) Dubbs silt loam, and (E) Sharkey clay.

well with the depth of wetting as determined from visual inspection by dismantling the samples for three of the five soils tested (Fig. 3, Table 2). The two samples that did not agree very well, not as closely as the other three soils, were the Grenada silt loam (Fig. 3B) and the Dubbs silt loam (Fig. 3D). In these cases, the depth of wetting was somewhat deeper than the cavities made by the penetrometer (Fig. 2A and 2C). The mean difference between penetrometer measurements taken immediately after the cessation of simulated rainfall and visual measurements taken after dismantling the cylinder containing the Grenada silt loam was 4 mm, with a standard deviation of 1.55 mm and 95% confidence limits of ±2.49 mm. For the Dubbs silt loam, the mean difference was 3.8 mm, the standard deviation was 1.57 mm, and 95% confidence limits were ±2.53 mm. Table 2 presents the mean wetting front depths measured with the penetrometer and by visual inspection for each of the cylinder tests. A statistical test (*t*-test) was performed (Table 2) to determine if the difference between the mean penetration depth and mean visual depth was statistically different and there was no significant statistical difference in the means of these measurements. The difference in visual and penetration wetting depths for these two cases may be in part attributed to an advance in wetting front depth between the time the penetrometer measurements were made and the sample was dismantled. The delay time between simulated rainfall cessation and soil removal was approximately 0.5 h.

The surface-protected sample was used to evaluate the effectiveness of the method in describing wetting front variations in the profile. The surface elevation and depth of penetration measurements are presented in Fig. 4. The results show a curvilinear wetting front extending from the edge of the protective filter strip to the cylinder wall, and an increase in the depth of the wetting front beneath the protective filter strip. Figure 2E presents the data from the same soil without the protective filter strip. The depth of wetting beneath the protective filter strip was twice the depth of wetting in the unprotected case. Also, the surface elevation beneath the filter strip was notably higher than the surface elevation away from the protective filter strip near the wall of the cylinder. Figure 2E shows similar data for the same soil without a protective filter strip. The surface elevation was uniform. By preventing seal formation, higher mean infiltration rates were maintained below the filter strip during rainfall simulation. Visual inspection corroborated these findings.

Penetrometer measurements in the large box with the swelling clay soil (Sharkey clay) are presented in Fig. 5. The mea-

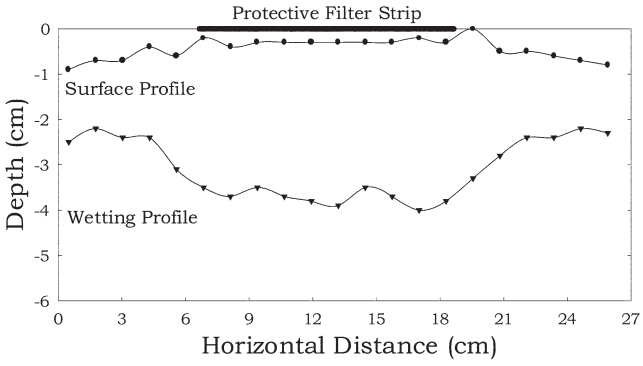

Fig. 4. Normalized surface elevation and penetration measurements of a Sharkey clay soil that had a protective filter strip placed on the surface before simulated rainfall.

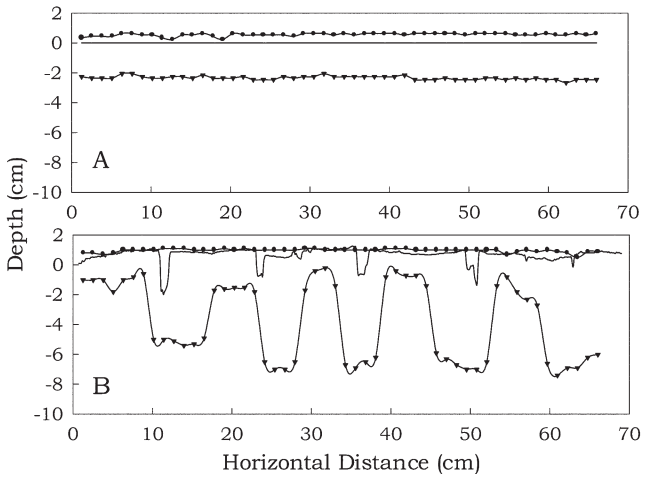

Fig. 5. Normalized surface elevation and penetration measurements from a series of simulated rainfall events with a Sharkey clay soil: (A) after the first simulated rainfall, and (B) after the third simulated rainfall. The solid line represents the surface elevation before the simulated rainfall, the solid line with solid circle symbols represents the surface elevation immediately after the simulated rainfall before penetration, and the solid line with solid triangle symbols represents the final penetration depth.

surements from the first simulated rainfall (initial uniformly packed sample with no cracks) did not indicate an irregular wetting front depth (Fig. 5A). Penetrometer measurements following the third simulated rainfall, Fig. 5B, showed wetting to be maximal in the neighborhood of the previous crack locations and minimal near the center of the previous prismatic soil peds (Wells et al., 2003). Within the prismatic soil ped, there was an inverted bowl shaped (convex) wetting front, derived from infiltration through the soil ped surface and lateral redistribution through the soil ped walls. As the soil surface began to dry, the centers of the previous prismatic soil peds, areas where the penetration measurement was minimal, became the focal point of crack development (Wells et al., 2003).

The primary limitation of the method is that it is a laboratory technique designed for measuring infiltration depths within packed soils. At this time, no measurements have been performed to study its usefulness with field soils, which can have large biological heterogeneities (worm holes, roots, etc.), as well as antecedent moisture conditions. Obviously, as the initial water content increases (from air dry), then the ability to detect differences in penetration resistance at the wetting front will decline. This limitation is probably dependent on soil texture; however, at this time we cannot validate these statements.

CONCLUSIONS

The miniature penetrometer approach was very successful in capturing the depth of wetting in three of five field soils tested, while the remaining soils offered very reasonable approximations. The technique was specifically designed to capture uneven or irregular wetting front surfaces in studies involving swelling clay soils that form cracks on drying. The reliability of the apparatus in experiments involving swelling clay soils permitted examination of the wetting depth near cracks and near the centers of prismatic columns.

REFERENCES

ASAE. 2006. Soil cone penetrometer S313.3. p. 902–904. *In* ASAE Standards. ASAE, St Joseph, MI.

Crestana, S., S. Mascarenhas, and R.S. Pozzi-Mucelli. 1985. Static and dynamic three-dimensional studies of water in soil using computed tomographic scanning. Soil Sci. 140:326–332.

DiCarlo, D.A., T.W.J. Bauters, T.S. Steenhuis, J.-Y. Parlange, and B.R. Bierck. 1997. High-speed measurements of three-phase flow using synchrotron x-rays. Water Resour. Res. 33:569–576.

Fellner-Feldeg, H. 1969. The measurement of dielectrics in the time domain. J. Phys. Chem. 73:616–623.

Hillel, D. 1980. Stress–strain relations and soil strength. p. 347–351. *In* Fundamentals of soil physics. Academic Press, New York.

Knight, J.H. 1992. Sensitivity of time domain reflectometry measurements to lateral variations in soil water content. Water Resour. Res. 28:2345–2352.

Lawless, G.P., N.A. MacGillivray, and P.R. Nixon. 1963. Soil moisture interface effects upon readings of neutron moisture probes. Soil Sci. Soc. Am. Proc. 27:502–507.

Liu, Y., B.R. Bierck, J.S. Selker, T.S. Steenhuis, and J.-Y. Parlange. 1993. High intensity x-ray and tensiometer measurements in rapidly changing preferential flow fields. Soil Sci. Soc. Am. J. 57:1188–1192.

Meyer, L.D., and W.C. Harmon. 1979. Multiple-intensity rainfall simulator for erosion research on row sideslopes. Trans. ASAE 22:100–103.

Nofziger, D.L. 1978. Errors in gamma-ray measurements of water content and bulk density in non-uniform soils. Soil Sci. Soc. Am. J. 42:845–850.

Perumpral, J.V. 1987. Cone penetrometer applications: A review. Trans. ASAE 30:939–944.

Petrovic, A.M., J.E. Siebert, and P.E. Rieke. 1982. Soil bulk density analysis in three dimensions by computer tomographic scanning. Soil Sci. Soc. Am. J. 46:445–450.

Reginato, R.J., and R.D. Jackson. 1971. Field measurement of soil-water content by gamma-ray transmission compensated for temperature fluctuations. Soil Sci. Soc. Am. Proc. 35:529–533.

Römkens, M.J.M., J.Y. Wang, and R.W. Darden. 1988. A laser microreliefmeter. Trans. ASAE 31:408–413.

Tackett, J.L., and R.W. Pearson. 1965. Some characteristics of soil crusts formed by simulated rainfall. Soil Sci. 99:407–413.

Tollner, E.W., J.W. Davis, and B.P. Verna. 1989. Managing errors with x-ray computed tomography (x-ray CT) when measuring physical properties. Trans. ASAE 32:1090–1096.

Topp, G.C., J.L. Davis, and A.P. Annan. 1980. Electromagnetic determination of soil water content: Measurements in coaxial transmission lines. Water Resour. Res. 16:574–582.

Topp, G.C., J.L. Davis, and A.P. Annan. 1982. Electromagnetic determination of soil water content using TDR: I. Applications to wetting fronts and steep gradients. Soil Sci. Soc. Am. J. 46:672–678.

van Bavel, C.H.M., D.R. Nielsen, and J.M. Davidson. 1961. Calibration and characteristics of two neutron moisture probes. Soil Sci. Soc. Am. Proc. 25:329–334.

van Bavel, C.H.M., N. Underwood, and S.R. Ragar. 1957. Transmission of gamma radiation by soils and soil densitometry. Soil Sci. Soc. Am. Proc. 21:588–591.

Wells, R.R., D.A. DiCarlo, T.S. Steenhuis, J.-Y. Parlange, M.J.M. Römkens, and S.N. Prasad. 2003. Infiltration and surface geometry features of a swelling soil following successive simulated rainstorms. Soil Sci. Soc. Am. J. 67:1344–1351.